IROS 95

Identifying Contact Formations in the Presence of Uncertainty*

A. O. Farahat B. S. Graves J. C. Trinkle

Department of Computer Science
Texas A&M University
College Station, TX, 77843-3112

Abstract

The efficiency of the automatic execution of complex assembly tasks can be enhanced by the identification of the contact state. In this paper we derive a new method for testing a hypothesized contact state using force sensing in the presence of sensing and control uncertainty. The hypothesized contact state is represented as a collection of elementary contacts. The feasibility of the elementary contacts is tested by solving a linear program. No knowledge of the contact pressure distribution or of the contact forces is required, so our method can be used even when the contact forces are statically indeterminate. We give a geometric interpretation of the contact identification problem using the theory of polyhedral convex cones. If more than one contact state is feasible, we use the geometric interpretation to determine the likelihood of each feasible contact formation.

1 Introduction

In this paper, we present a linear programming approach to the force/moment testing of the different contact topologies. This approach yields two benefits over the previous techniques: no estimate of the pressure distribution in the contact interface is required, and the contact formation can be identified even when the contact forces are statically indeterminate.

The work presented here extends that of Xiao [1], on contact identification, Desai [2], who introduced the concept of contact formation and sensor-based recognition of contact formations, Hirai and Asada [3], who used Monte Carlo techniques to develop contact formation classifiers from a CAD model, and of Taylor [4] and Brooks [5] on spatial and force uncertainty.

Consider a movable polyhedral object $\mathcal{W}$, which is held by a robot, contacting polyhedron obstacles $\mathcal{E}$. The forces and moments acting on the movable object can be measured by a force sensor. The exact contact formation is not known. The problem to be solved can be stated as: *given a set of measured forces and moments, a set of hypothetical contact formations, and an uncertainty model, find the contact formation.*

*This research was supported by the National Science Foundation (grant IRI-9304734), the Texas Advanced Research Program (999903-078), and the Texas Advanced Technology Program (999903-095).

We make the following assumptions:

1. The bodies in the system are rigid polyhedra,
2. Friction forces obey Coloumb's Law,
3. Force/moment sensing errors are bounded,
4. No uncertainty exists in the model of the environment,
5. The position and orientation of the robot are specified.

The first four assumptions are commonly made in analyses of robotic manipulation systems and experimental results support their validity.

The last assumption does not exclude uncertainty in the location of robot. The uncertainty in the location of the robot is handled by the first phase of the contact formation identification algorithm: the hypothesis phase. In the hypothesis phase, we use Xiao's algorithm to obtain a discrete set $\mathcal{D}_s$ of possible locations of the robot and a list of possible contact formations corresponding to each element of $\mathcal{D}_s$. Each element of $\mathcal{D}_s$ along with the list of possible contact formations is then passed to the testing phase of the contact identification algorithm.

2 Contact Models

For simplicity we consider contacts between two polyhedra. Let $\mathcal{W}$ denote the movable object and $\mathcal{E}$ denote the polyhedral environment. The contacts can be described in terms of three *elementary* types of contacts [6]

Type A between a face of $\mathcal{W}$ and a vertex of $\mathcal{E}$.

Type B between a vertex of $\mathcal{W}$ and a face of $\mathcal{E}$.

Type C between an edge of $\mathcal{W}$ and an edge of $\mathcal{E}$.

3 Uncertainty Models

The most important sources of uncertainty are: uncertainty in the force/moment sensor, uncertainty in the positions of the contact points with respect to the force sensing frame, the uncertainty in the direction of the contact normal with respect to the force sensing

0-8186-7108-4/95 $4.00

frame, and the uncertainty in the position and orientation of the force sending frame with respect to a world frame. All but the first source of uncertainty are handled by the first phase of the contact identification algorithm.

Let S be the force sensor internal coordinate frame. Let C be a coordinate frame attached to the object's center of gravity and aligned with the world frame $\mathcal{W}$. For the rest of this paper we use "generalized force" to imply force and moment. Let $\mathbf{g}_S$ denote the actual generalized force applied at frame S, and let $\hat{\mathbf{g}}_S$ denote the measured value for the generalized force. Also, let $\delta\mathbf{g}_S$ be the vector of uncertainty in the force sensing given by:

$$\delta\mathbf{g}_S = [\ \delta g_{S_x}\quad \delta g_{S_y}\quad \delta g_{S_z}\quad \delta g_{S_\alpha}\quad \delta g_{S_\beta}\quad \delta g_{S_\gamma}\ ]^T \tag{1}$$

Thus:

$$\hat{\mathbf{g}}_S - \delta\mathbf{g}_S < \mathbf{g}_S < \hat{\mathbf{g}}_S + \delta\mathbf{g}_S. \tag{2}$$

The above inequality applies element by element. Let the homogeneous transform from S to C be given by

$$\mathbf{T} = \begin{bmatrix} R_{11} & R_{12} & R_{13} & x_1 \\ R_{21} & R_{22} & R_{23} & y_1 \\ R_{31} & R_{32} & R_{33} & z_1 \\ 0 & 0 & 0 & 1 \end{bmatrix} \tag{3}$$

Let $\mathbf{R}$ denote the 3×3 rotational component of $\mathbf{T}$ and $\mathbf{P}$ the 3×1 translational component of $\mathbf{T}$. The generalized forces acting at C are given by:

$$\mathbf{g}_C = {}^C_S\mathbf{T}_f \mathbf{g}_S \tag{4}$$

where ${}^C_S\mathbf{T}_f$ is the 6×6 force transformation associated with $\mathbf{T}$ [7].

The sensed forces acting at C are given by:

$$\hat{\mathbf{g}}_C = {}^C_S\mathbf{T}_f \hat{\mathbf{g}}_S \tag{5}$$

It should be noted that the force transformation matrix ${}^C_S\mathbf{T}_f$ is deterministic since it corresponds to an element of the discrete set $\mathcal{D}_s$ of possible locations given by Xiao's algorithm.

Expanding Equations (4) and (1) we get:

$$g_{C_x} = R_{11}g_{S_x} + R_{12}g_{S_y} + R_{13}g_{S_z} \tag{6}$$

$$\delta g_{C_x} = R_{11}\delta g_{S_x} + R_{12}\delta g_{S_y} + R_{13}\delta g_{S_z} \tag{7}$$

where δg_{C_x} is the error in the first component of transformed measurement. $\delta\mathbf{g}_C$ is the transformed measurement error vector.

Using the error bounds on g_x, g_y, and g_z we can identify the maximum and minimum values of g_{C_x}. Denote those values by $g_x{}^+$ and $g_x{}^-$ respectively.

$$g_x{}^- \le g_{C_x} \le g_x{}^+ \tag{8}$$

$$g_x{}^+ = |R_{11}\delta g_{S_x}| + |R_{12}\delta g_{S_y}| + |R_{13}\delta g_{S_z}| \tag{9}$$

$$g_x{}^- = -|R_{11}\delta g_{S_x}| - |R_{12}\delta g_{S_y}| - |R_{13}\delta g_{S_z}| \tag{10}$$

Similar bounds can be obtained for the other components of the generalized force vector $\mathbf{g}_C$. All the bounds can be written as:

$$\mathbf{g}_C{}^- < \mathbf{g}_C < \mathbf{g}_C{}^+ \tag{11}$$

where $\mathbf{g}^- = [g_x{}^-, g_y{}^-, ...]^T$ with $\mathbf{g}^+$ defined similarly.

Equation (11) represents a rectangular solid in generalized force space centered around the nominal generalized forces at C $\hat{\mathbf{g}}_C$ that bounds the actual generalized force $\mathbf{g}_C$ at C.

4 Model Description

When a frictionless rigid body is in contact with its environment, the effect of the contact forces and the external forces must balance. Let $\dot{\mathbf{q}}$ denote the velocity of the center of gravity of the object in the world frame and $\dot{\theta}$ denote the joint rates of the polyhedral obstacles. Let $\mathbf{c}_n$ denote the vector of contact wrench intensities. The following equations represent the kinematic and equilibrium constraints that must be satisfied if the object is stationary or moving quasi-statically while maintaining the contact formation [8]:

$$\mathbf{W}_n{}^T\dot{\mathbf{q}} + \mathbf{J}_n\dot{\theta} = 0 \tag{12}$$

$$\mathbf{W}_n\mathbf{c}_n = -\mathbf{g}_{obj} \tag{13}$$

$$\mathbf{c}_n \ge 0 \tag{14}$$

where $\mathbf{g}_{obj}$ is the external wrench acting on the object and $\mathbf{J}_n$ is the Jacobian of the polyhedral obstacles. Let $\hat{\mathbf{n}}_j$ be the unit normal at the contact point j expressed in frame C, and $\mathbf{r}_j$ be the vector from the origin of frame C to contact point j. The wrench matrix $\mathbf{W}_n$ [9] is given by :

$$\mathbf{W}_n = \begin{bmatrix} \hat{\mathbf{n}}_1 & \hat{\mathbf{n}}_2 & \dots & \hat{\mathbf{n}}_l \\ \mathbf{r}_1 \wedge \hat{\mathbf{n}}_1 & \mathbf{r}_2 \wedge \hat{\mathbf{n}}_2 & \dots & \mathbf{r}_l \wedge \hat{\mathbf{n}}_l \end{bmatrix} \tag{15}$$

where $\wedge$ is the cross product operator and l is the number of contacts.

In the case that the polyhedral obstacles are not moving Equation (12) reduces to

$$\mathbf{W}_n{}^T\dot{\mathbf{q}} = 0 \tag{16}$$

The instantaneous velocity of the center of gravity of the object is related to the manipulator's joint rates $\dot{\theta}_m$ by :

$$\dot{\mathbf{q}} = \mathbf{J}_m\dot{\theta}_m \tag{17}$$

where $\mathbf{J}_m$ is the manipulator Jacobian matrix. Substituting equation (17) into equation (16) we get :

$$\mathbf{W}_n{}^T\mathbf{J}_m\dot{\theta}_m = 0 \tag{18}$$

The null space of $\mathbf{W}_n{}^T\mathbf{J}_m$ is the space of manipulator joint rates $\dot{\theta}_m$ for which the current contact formation is maintained as the robot moves. The null space of $\mathbf{J}_m$ correspond to motions of the manipulator for which the object is motionless. Denote the union of the two null spaces by $\dot{\theta}_{m_v}$.

A contact formation is force-feasible if it is possible to find contact forces that satisfy equilibrium, friction, and other kinematic constraints. To test whether a contact formation is force-feasible it is sufficient to test whether Equations (13) & (14) are feasible. This can

be easily tested using the feasibility test of the linear program:

$$\underset{\mathbf{c}_n}{Minimize} \quad 0 \tag{19}$$

$$Subject\ to: \quad \mathbf{W}_n\mathbf{c}_n = -\mathbf{g}_{obj} \tag{20}$$

$$\mathbf{c}_n \geq 0 \tag{21}$$

It should be noted that the LP can be used if the manipulator's joint rates are either zero or in the range $\dot{\theta}_{mv}$. It then follows that for all joint rates in the range $\dot{\theta}_{mv}$, the contact formation is feasible if and only if the corresponding linear program is feasible.

In formulating the wrench matrix we use the position and orientation of the object corresponding to the element of $\mathcal{D}_s$ being tested to get $\mathbf{r}_j$ and $\hat{\mathbf{n}}_j$. This method of discretizing the location uncertainty of the object and then testing the elements of the discrete set $\mathcal{D}_s$ ensures that the feasibility of the contact formation always corresponds to the feasibility of a *linear model*. In the absence of such a discretization, the uncertainty in the wrench will lead to a nonlinear model. A contact formation will be feasible if it is possible to find $\mathbf{c}_n$ and $\mathbf{g}_{obj}$ that satisfy the equilibrium condition (13) and the physical condition (14), such that $\mathbf{g}_{obj}$ also satisfies the error model (11).

In this spirit we modify the linear program (19) to the following linear program:

$$\underset{\mathbf{c}_n, \mathbf{g}_{obj}}{Minimize} \quad 0 \tag{22}$$

$$Subject\ to: \quad \mathbf{W}_n\mathbf{c}_n = -\mathbf{g}_{obj} \tag{23}$$

$$\mathbf{c}_n \geq 0 \tag{24}$$

$$\mathbf{g}^- \leq \mathbf{g}_{obj} \leq \mathbf{g}^+ \tag{25}$$

In the case of friction the above analysis must be modified. Friction will impact our model in two ways. First, the wrench matrix will also include unit wrenches due to frictional forces in the contact plane. Second, the Coloumb friction model will be included as an extra set of constraints. Let $\hat{\mathbf{t}}_j$ and $\hat{\mathbf{o}}_j$, denote a pair of orthonormal vectors in the contact plane. The wrench matrix can be written as: $\mathbf{W} = [\mathbf{W}_n\ \mathbf{W}_t\ \mathbf{W}_o]$ where $\mathbf{W}_n$ is given by equation (15). $\mathbf{W}_t$ and $\mathbf{W}_o$ can be obtained by replacing $\hat{\mathbf{n}}_j$ in equation (15) with $\hat{\mathbf{t}}_j$ and $\hat{\mathbf{o}}_j$ respectively.

The wrench intensity vector $\mathbf{c}$ is given by:

$$\mathbf{c}^T = [\mathbf{c}_n^T \mathbf{c}_t^T \mathbf{c}_o^T] \tag{26}$$

where $\mathbf{c}_n$ is the vertical concatenation of the wrench intensities in the normal direction. $\mathbf{c}_t$ and $\mathbf{c}_o$ are similarly defined. The Coloumb Friction Law is applied by the nonlinear inequality:

$$c_{t_j}{}^2 + c_{o_j}{}^2 \leq \mu_j c_{n_j}{}^2 \tag{27}$$

Where μ_j is the static coefficient of friction at the j_{th} contact point. The nonlinear inequality (27) corresponds to a friction cone which can be approximated by an $m - sided$ inscribed pyramid. The inscribed pyramid gives a conservative approximation of the friction cone.

The approximation of the Coloumb Law may be written as the following linear constraints [10]:

$$\mathbf{B}\mathbf{c} \geq 0 \tag{28}$$

If the external load at the center of gravity of the object is not precisely known, then the linear program (22) is augmented with the error model (11) to yield:

$$\underset{\mathbf{c}_n, \mathbf{g}_{obj}}{Minimize} \quad 0 \tag{29}$$

$$Subject\ to: \quad \mathbf{W}\mathbf{c} = -\mathbf{g}_{obj} \tag{30}$$

$$\mathbf{g}^- < \mathbf{g}_{obj} < \mathbf{g}^+ \tag{31}$$

$$\mathbf{B}\mathbf{c} \geq 0 \tag{32}$$

If the linear program (29) is feasible, then it is possible to find contact forces that satisfy the equilibrium conditions and the Coloumb model, and external forces that satisfy the equilibrium model and the sensing model.

5 Contact Formation Likelihood

In this next section we propose a computational procedure to determine the most likely contact formation. Equations (30) and (32) define a polytope in wrench space. Let $\mathcal{G}_i$ denote the polytope corresponding to contact formation i. The measurement and the bounds on the measured force equation (31) define a box $\mathcal{G}_f$ of possible wrench vectors. If a contact formation i is feasible, then the intersection of the polytope corresponding to that contact and $\mathcal{G}_f$ is non empty. This is illustrated in Figure 1 which shows two feasible contact formations i and j. The two dark areas represent the intersection of $\mathcal{G}_f$ with $\mathcal{G}_i$ and $\mathcal{G}_j$.

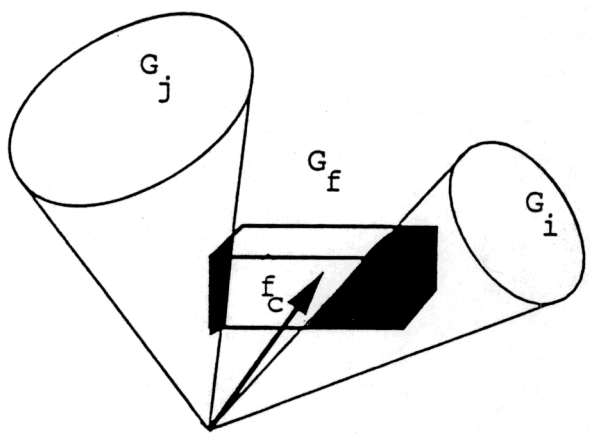

Figure 1: Intersection of $\mathcal{G}_f$ and $\mathcal{G}_i$, $\mathcal{G}_j$

5.1 Quadratic Programming Approach

As mentioned above, external wrench vectors $\mathbf{g}_{obj}$ satisfying the linear program (29) corresponding to

contact formation i form a polytope $\mathcal{G}_{if}$ in force space. In fact this polytope is given by

$$\mathcal{G}_{if} = \mathcal{G}_i \cap \mathcal{G}_f \tag{33}$$

The two dark regions of Figure 1 represent $\mathcal{G}_{if}$ and $\mathcal{G}_{jf}$. We define d_{min}, the minimum distance from $\mathcal{G}_{if}$ to the sensed force $\hat{\mathbf{g}}_C$ by

$$d_{min} = min\{d(\mathbf{x}) | \mathbf{x} \in \mathcal{G}_{if}\} \tag{34}$$

Where $d(\mathbf{x})$ is the weighted Euclidian distance of a vector $\mathbf{x}$ from $\hat{\mathbf{g}}_C$. The minimum distance, d_{min}, is the solution to the following positive definite quadratic program:

$$\begin{aligned}
&\underset{\mathbf{c}_n, \mathbf{g}_{obj}}{Minimize} && [\hat{\mathbf{g}}_C - \mathbf{g}_{obj}]^T \mathbf{Q} [\hat{\mathbf{g}}_C - \mathbf{g}_{obj}] && (35)\\
&Subject\ to: && \mathbf{W}_n \mathbf{c}_n = \mathbf{g}_{obj} && (36)\\
& && \mathbf{c}_n \geq 0 && (37)\\
& && \mathbf{g}^- < \mathbf{g}_{obj} < \mathbf{g}^+ && (38)\\
& && \mathbf{B}\mathbf{c} \geq 0 && (39)
\end{aligned}$$

where $\mathbf{Q}$ is a (6×6) diagonal matrix.

If contact formation i is feasible as indicated by the feasibility of the linear program (29) , then $\mathcal{G}_{if}$ is non empty. In this case the quadratic program has a unique global minimum. If d_{min} is zero, then the sensed force is in $\mathcal{G}_i$. The feasible contact formations are ranked according to their d_{min} values.

The above procedure will break down if the sensed force is in more than one of the $\mathcal{G}_i$. In the next subsection we develop a procedure to handle this case.

5.2 Probabilistic approach

If the sensed force is in $\mathcal{G}_i ... \mathcal{G}_{i+s}$ we can compute the probability that a contact formation i is feasible by computing the probability that the actual force is in the $\mathcal{G}_i$. In this subsection we show how to compute this probability from the sensor error model.

The sensed force $\hat{\mathbf{g}}_C$ differs from the actual force $\mathbf{g}_C$ by a random error vector $\delta \mathbf{g}_C$. In Section 3 we obtained expressions for the components of $\delta \mathbf{g}_C$ in terms of the components of the vector of sensed force errors and the homogeneous transform $\mathbf{T}$. The probability density functions of the components of $\delta \mathbf{g}_C$ can be obtained from those expressions and the sensed force error statistics. For a given sensed force $\hat{\mathbf{g}}_C$ we define a discrete set $\mathcal{F}$ of cardinality N by:

$$\mathcal{F} = \{\mathbf{x} | \mathbf{x} = \hat{\mathbf{g}}_C + \delta \mathbf{g}_C\} \tag{40}$$

where $\mathcal{F}$ is a set of possible actual forces.

If an element of $\mathcal{F}$ is a member of $\mathcal{G}_i$, then the contact formation i is feasible. If all the elements of $\mathcal{F}$ are in $\mathcal{G}_i$, then contact formation i is very likely. If none of the elements of $\mathcal{F}$ are in $\mathcal{G}_i$, then contact formation i is not likely. Let p_i represent the number of elements of $\mathcal{F}$ in $\mathcal{G}_i$. Also define the operator $conf()$ by : $conf(\mathcal{G}_i) = \frac{n_i}{N}$ $conf(\mathcal{G}_i)$ is a measure of the set $\mathcal{G}_i \cap \mathcal{F}$.

Next we state and prove a proposition that will be useful in the computation of the confidence measure:

Proposition 1: *Let $\mathcal{U} = span\{\mathbf{u}_1 \cdots \mathbf{u}_l\}$ be a convex polyhedral cone in $\mathcal{R}_n$. Let $\mathbf{W}$ be a linear map from $\mathcal{R}_n$ to $\mathcal{R}_m$. Then*

$$\mathbf{W}\mathcal{U} = span\{\mathbf{W}\mathbf{u}_1 \cdots \mathbf{W}\mathbf{u}_n\} \tag{41}$$

and $\mathbf{W}\mathcal{U}$ is a polyhedral convex cone.

Proof:

$$\begin{aligned}
\mathcal{U} &= \{a_1\mathbf{u}_1 + a_2\mathbf{u}_2 + \cdots + a_n\mathbf{u}_n\} && (42)\\
\mathbf{W}\mathcal{U} &= \{a_1\mathbf{W}\mathbf{u}_1 + \cdots a_n\mathbf{W}\mathbf{u}_n\} && (43)\\
&= span\{\mathbf{W}\mathbf{u}_1 \cdots \mathbf{W}\mathbf{u}_n\} && (44)
\end{aligned}$$

Since $a_1 \cdots a_n > 0$, it follows that $\mathbf{W}\mathcal{U}$ is also a polyhedral convex cone. ..... □

To determine if an element of $\mathcal{F}$ is a member of $\mathcal{G}_i$, we propose the following algorithm:

1. Transform the system of inequalities $\mathbf{B}\mathbf{c} \geq 0$ from face form to span form [3] :

$$\mathbf{B}\mathbf{c} \geq 0 \Longrightarrow span\{\mathbf{d}_1 \cdots \mathbf{d}_m\} \tag{45}$$

2. Apply the linear transformation $\mathbf{W}$ to $\mathbf{d}_1 ... \mathbf{d}_n$ to get

$$\mathcal{G}_i = span\{\mathbf{h}_1 \cdots \mathbf{h}_m\} \tag{46}$$

From the previous proposition, $\mathcal{G}_i$ is a polyhedral convex cone.

3. Transform the polyhedral convex cone (46) from span form to face form [3].

$$span\{\mathbf{h}_1 \cdots \mathbf{h}_m\} \Longrightarrow \mathbf{G}_i\mathbf{x} \leq 0 \tag{47}$$

4. If a vector $\mathbf{x}$ in $\mathcal{F}$ is in $\mathcal{G}_i$ the equation (47) must be satisfied.

The set $\mathcal{F}$ is computed only once and thus the time required to compute it is independent of the number of contact formations to be tested. The face form representation of the polytope of possible wrench forces $\mathcal{G}_i$ is done only once for contact formation i. Efficient methods have been developed by Hirai [3] and Hirukawa [11] for performing this transformation. Once the face form is obtained, it is possible to test if an element g_p of $\mathcal{F}$ is a member of $\mathcal{G}_i$ by checking the sign of $\mathcal{G}_i g_p$.

It is possible to test if $\mathbf{g}_p \in \mathcal{F}$ is a member of $\mathcal{G}_i$ by testing the feasibility of the linear program:

$$\begin{aligned}
&\underset{\mathbf{c}_n}{Minimize} && 0 && (48)\\
&Subject\ to: && \mathbf{W}\mathbf{c} + \mathbf{g}_p = 0 && (49)\\
& && \mathbf{B}\mathbf{c}_n \geq 0 && (50)
\end{aligned}$$

The procedure outlined in this subsection offers considerable computational savings for a large N. If a linear program is used, we need to test the feasibility of N linear programs. Using the procedure outlined in this section only 2 linear programs and N matrix-vector multiplications are needed.

If the confidence measure can not be computed using the above approach due to computational constraints then we propose the following linear programming alternative:
Since $\hat{g_C}$ lies in all $\mathcal{G}_i, i = 1 \cdots s$ it follows that $v_i = G_i \hat{g_C} \leq 0, i = 1 \cdots s$. The value of v_i can be used as a measure of $\mathcal{F} \cap \mathcal{G}_i$, $i = 1..s$. A large negative value of v_i indicates that the contact formation is likely. The same approach was used by Trinkle [12] to formulate a quantitative test for form closure.

It should be noted that the probabilistic approach gives more accurate results since it uses the actual sensor error statistics.

5.3 Identification Algorithm

We have shown that if the nominal force measurement $\hat{g_C}$ happens to lie in the polyhedral convex cone $\mathcal{G}_i$ then the measure of $\mathcal{G}_i \cap \mathcal{F}$ will greater than had it not. This suggests that we can initially test to see if $\hat{g_C}$ happens to lie in any of the possible $\mathcal{G}_i, i = 1...k$ where k is the number of possible contact formations. The outcome of this test can be one of the following: a) $\hat{g_C}$ does not lie in any of polyhedral convex cones. In this case we have to test whether the polytope $\mathcal{F}$ intersects any $\mathcal{G}_i$. b) $\hat{g_C}$ lies in more than one of the polyhedral convex cones. In this case all of the contact formations corresponding to those polyhedral convex cones are possible and we have to calculate the confidence measure of each of those cones. c) $\hat{g_C}$ lies in one of the polyhedral convex cones. The most likely contact formation is the contact formation corresponding to this cone.

The feasibility of the following linear program may be used to test whether $\hat{g_C}$ lies inside any of the polyhedral convex cones:

$$\begin{aligned} &Minimize && 0 && (51)\\ &Subject\ to: && \mathbf{W}\mathbf{c} = \mathbf{g}_{obj} && (52)\\ &&& \mathbf{B}\mathbf{c}_a \geq 0 && (53) \end{aligned}$$

where W and B correspond to the contact formation to be tested. The feasibility of this linear program is easier to check than the feasibility of the linear program (22) for two reasons. First, it does not require any knowledge of the bounds on $\hat{g_C}$, so the overhead involved in computing those bounds is avoided. Second, 6 fewer variables are needed.

In light of the the above discussion, we implemented the following procedure for identifying the contact formation:

- If $\hat{g_C}$ lies in only one of the polyhedral convex cones, return the contact formation corresponding to that cone.
- If $\hat{g_C}$ lies in none of the polyhedral convex cones, use the method of Section 5.1. Rank the contact formations according to the values of d_{min}.
- If $\hat{g_C}$ lies in s polyhedral convex cones with $s > 1$, test the measure of $\mathcal{F} \cap \mathcal{G}_i, i = 1 \cdots s$ using the method of Section 5.2.

6 Results

The contact formation identification technique described here was tested in the laboratory. The software was written in the C programming language running on an IBM RS6000 workstation. The linear programs were solved using the IMSL [13] library. The hardware system consisted of a PUMA 560 robot, a JR3 force/moment sensor, and a pneumatic gripper.

Our robot controller is implemented using RCCL [14] running under LynxOS [15] on an 486-based microcomputer. Communication between our robot controller and the RS6000 is handled by the TelRIP telerobotics communication package [16].

The workpiece used for our test was a rectangular aluminum peg and the environment consisted of a solid plate of aluminum. Figure 2 shows the system used.

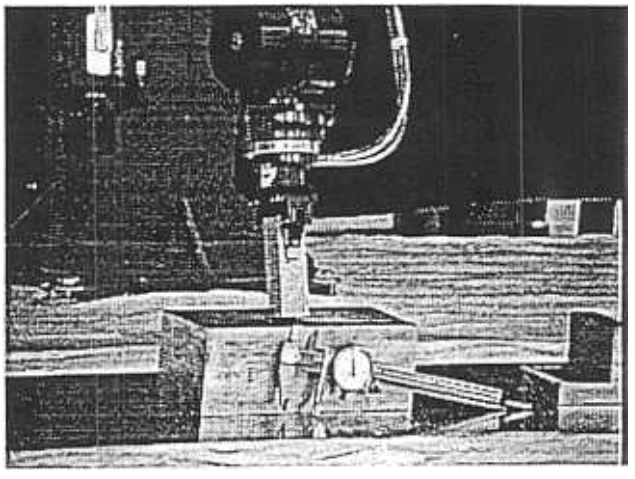

Figure 2: The experimental setup.

The first contact we tested was a face-face contact. The measured forces and moments are shown in the second column of Table 1.

The first contact formation to be hypothesized and tested was a face-face contact modeled as a $4A$ contact formation. Initially the feasibility test for the contact formation assumed perfect sensing using the linear program (51). The feasibility test was performed in 0.03 CPU seconds. The linear program was not feasible. Next we tested the feasibility of the linear program (22). The error bounding box is given in the second column of Table 2. The feasibility of the linear program was tested in 0.04 CPU seconds. The linear program was feasible.

Due to the uncertainty in the position of the peg an edge-face contact is also possible. An edge-face contact could be obtained by rotating the face-face configuration by the XYZ Euler angles $(0, \delta\beta, 0)$, where $\delta\beta$ is a small angle that represents the uncertainty in the orientation. The edge-face contact formation was modeled as a $2A$ contact formation and the corresponding linear program was formulated. We tested the feasibility of the linear program for $\delta\beta = 0.001$, which took 0.02 CPU seconds. The program was not feasible.

A vertex-face configuration could also be obtained by rotating the face-face configuration by the

Parameter	Face-Face	Vertex-Face
$\hat{gc}_x$	-2.3763 N	0.2225 N
$\hat{gc}_y$	-0.9345 N	0.5607 N
$\hat{gc}_z$	-38.9998 N	-17.1993 N
$\hat{gc}_\alpha$	2.3798 Ncm	73.5517 Ncm
$\hat{gc}_\beta$	11.4358 Ncm	20.3376 Ncm
$\hat{gc}_\gamma$	8.1665 Ncm	3.1301 Ncm

Table 1: Measured force and moments.

Parameter	Face-Face	Vertex-Face
δgc_x	0.0445 N	0.0447 N
δgc_y	0.0445 N	0.0563 N
δgc_z	0.0445 N	0.0458 N
δgc_α	1.356 Ncm	1.3609 Ncm
δgc_β	1.356 Ncm	1.7165 Ncm
δgc_γ	1.356 Ncm	1.7192 Ncm

Table 2: Force sensing error bounds.

XYZ Euler angles $(0, \delta\beta, \delta\gamma)$, where $\delta\beta, \delta\gamma$ are small angles that represent the uncertainty in the orientation. The vertex-face contact formation was modeled as an A contact formation and the corresponding linear program was formulated. We tested the feasibility of the linear program for $\delta\beta = 0.001$, $\delta\gamma = 0.001$, which took 0.01 CPU seconds, and the linear program was found to be not feasible.

Next we rotated the configuration of the robot to obtain the vertex-face contact formation. The measured forces and moments are given in the third column of Table 1. The uncertainty in force sensing is given in the third column of Table 2. To test our approach we hypothesized a vertex-face contact modeled by a type A contact. The linear program was feasible and the run time in this case was 0.01 CPU seconds.

7 Conclusion

We have presented a new method for contact formation identification through force sensing, an error model that incorporates sensing errors and contact compliance, a linear programming algorithm, and three different methods for computing the confidence measure of a contact formation.

We illustrated the utility of our method by means of two examples. In both examples, the contacts were properly identified. The run time of this method was very satisfactory and indeed can be used in real time applications.

References

[1] J. Xiao and L. Zhang, "Towards obtaining all possible contacts- growing a polyhedron by its location uncertainty," *IEEE Trans. Robotics and Automation*, 1994. submitted.

[2] R. S. Desai, *On Fine Motion in Mechanical Assembly in Presence of Uncertainty.* PhD thesis, University of Michigan Department of Mechanical Engineering, Ann Arbor, MI, May 1989.

[3] S. Hirai and H. Asada, "Kinematics and statics of manipulation using the theory of polyhedral convex cones," *Int. J. Robotics Research*, vol. 12, no. 5, pp. 434–447, 1993.

[4] R. H. Taylor, *A Synthesis of Manipulator Control Programs from Task-Level Specification.* PhD thesis, Stanford University Department of Computer Science, Stanford, CA, July 1976.

[5] R. A. Brooks, "Symbolic reaoning among 3-d models and 2-d images," *Artificial Intelligence*, vol. 17, no. 1, pp. 285–348, 1981.

[6] J.-C. Latombe, *Robot Motion Planning.* Norwell, MA: Kluwer Academic Publishers, 1991.

[7] J. Craig, *Introduction to Robotics: Mechanics and Control.* Reading, MA: Addison-Wesley, second ed., 1989.

[8] J. Trinkle and D. Zeng, "Planar quasistatic motion of a lamina with uncertain contact friction," in *Proc. IEEE Int. Conf. Intelligent Robots and Systems*, pp. 1642–1649, 1992.

[9] H. Asada and A. B. By, "Kinematics of workpart fixturing," in *Proc. IEEE Int. Conf. Robotics and Automation*, pp. 337–345, March 1985.

[10] J. C. Trinkle, *The mechanics and planning of enveloping grasps.* PhD thesis, Univ. of Pennsylvania Department of Systems Engineering, Philadelphia, PA, June 1987.

[11] H. Hirukawa, T. Matsui, and K. Takase, "Automatic determination of possible velocity and applicable force of frictionless objects in contact from geometric model," *IEEE Trans. Robotics and Automation*, vol. 10, no. 3, pp. 309–322, 1994.

[12] J. Trinkle, "A quantitative test for form closure grasps," in *Proc. IEEE Int. Conf. Intelligent Robots and Systems*, pp. 1670–1677, 1992.

[13] IMSL, Inc., Houston, Texas, *C/Base/Library Version 1.0 Reference Manual*, January 1991.

[14] V. Hayward and R. Paul, "Robot manipulator control under UNIX: RCCL, a robot control C library," *Int. J. Robotics Research*, vol. 5, no. 4, pp. 94–111, 1986.

[15] Lynx Real-Time Systems, Inc., Los Gatos, CA, *LynxOS Version 2.2.1 Reference Manual*, July 1993.

[16] J. D. Wise and L. Ciscon, "Telrip distributed applications environment operating manual," Tech. Rep. 9103, Rice University, 1992. Universites Space Automation/Robotics Consortium.